Available online at www.eccomasproceedia.org
Eccomas Proceedia COMPDYN (2023) 961-970

ECCOMAS
Proceedia

COMPDYN 2023
9th ECCOMAS Thematic Conference on
Computational Methods in Structural Dynamics and Earthquake Engineering
M. Papadrakakis, M. Fragiadakis (eds.)
Athens, Greece, 12-14 June 2023

THREE-DIMENSIONAL FRAME ANALYSIS OF Q–Δ RESONANCE OF CENTER-CORE BIAXIALLY SYMMETRICAL HIGH-RISE BUILDING UNDER LONG-PERIOD EARTHQUAKE MOTION

Masayuki Kohiyama[1] **and Shiori Maki**[2]

[1] Department of System Design Engineering, Faculty of Science and Technology, Keio University
3-14-1 Hiyoshi, Kohoku-ku, Yokohama, 223-8522, Japan
kohiyama@sd.keio.ac.jp

[2] School of Science for Open and Environmental Systems, Graduate School of Science and Technology, Keio University
3-14-1 Hiyoshi, Kohoku-ku, Yokohama, 223-8522, Japan
oin11shiori@keio.jp

Abstract

When large displacements occur in buildings with different stiffnesses in the two horizontal directions, torsional moments are generated owing to geometric nonlinearities. Consequently, when the sum or difference of the translational mode natural frequencies in the two horizontal directions is close to the torsional mode natural frequency, the torsional mode is excited. This is known as Q–Δ resonance. Therefore, we created a three-dimensional frame model of a center-core high-rise building with a biaxially symmetrical plane that satisfied the Q–Δ resonance condition and examined whether the torsional response was excited by long-period design waves. A time-history response analysis was conducted assuming elastic response and considering geometric nonlinearities. It was confirmed that the torsional mode could be induced.

Keywords: High-Rise Building, Long-Period Ground Motion, Torsional Response, Geometric Nonlinearity, Q–Δ Resonance.

doi: 10.7712/120123.10449.21098

1 INTRODUCTION

The causes of torsional vibration of buildings under seismic excitation have been studied for more than half a century [1], the risk of asymmetric structures with eccentricity having been reported in many articles [2–4]. Moreover, the Japanese Building Standard Law makes provision for eccentricity, which represents the misalignment between the center of gravity and the rigid center of buildings. However, torsional response occurs in buildings without eccentricity owing to horizontal displacement and orthogonal inertial forces. The authors' research group [5] called this phenomenon the "*Q–Δ* effect" and analyzed the resonance phenomenon in which a torsional mode was induced when the natural frequency of the torsional mode matched the sum or difference of the natural frequencies of the translational modes in the two horizontal directions. This phenomenon was called "*Q–Δ* resonance." The *Q–Δ* effect was later redefined as a phenomenon in which—when the stiffnesses in the two horizontal directions were different—a simultaneous displacement in the two horizontal directions generated a torsional moment due to the interaction of bending and torsion caused by geometric nonlinearities [7] (**Fig. 1**). *Q–Δ* resonance has been the subject of theoretical investigations [8–11], shaking table experiments using test specimens [12–14], and analyses using finite element [7] and three-dimensional frame models [14].

Q–Δ resonance can have a particularly large effect on high-rise buildings, especially those in which large displacements occur in the upper floors due to long-period seismic motion. For example, in the event of a large Nankai Trough earthquake, which can be expected to cause long-period and long-duration seismic motion, there is a risk that long-period seismic motion could propagate over a wide area and cause extensive damage [15]. It is evident that the risk of *Q–Δ* resonance needs to be closely examined in light of the recent construction of super-high-rise buildings. Consequently, a three-dimensional frame model of a center-core high-rise building with a 320-m high outrigger belt truss that could generate *Q–Δ* resonance in the first torsional mode has been studied [14]. However, in real buildings [16], the second torsional mode is often close to the *Q–Δ* resonance condition. Therefore, in this study, a three-dimensional frame model of a 200-m tall center-core super-high-rise building was developed, and time-history response analysis was conducted to analyze the possibility of *Q–Δ* resonance of second torsional modes in super-high-rise buildings.

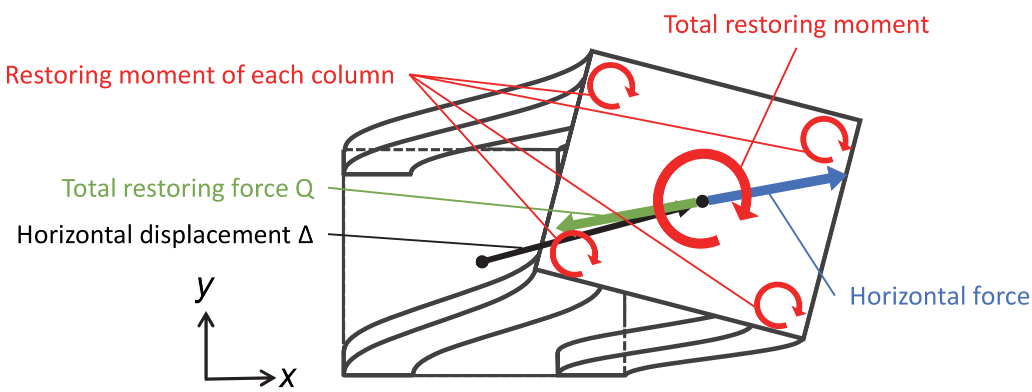

Figure 1: The *Q–Δ* effect.

2 ANALYTICAL MODEL OF A HIGH-RISE BUILDING

2.1 Overview of the model

Here, we present an overview of the structure of the target high-rise building. Previous studies [17] have pointed out that bending deformation of the entire building could reduce the torsional response due to *Q–Δ* resonance. Consequently, in this study the large height/width aspect ratio was specified to increase the bending deformation, and a center-core steel moment-resisting frame without a belt truss was used. The building was assumed to be a 50-story, 200-m high office building with a biaxially symmetrical plan without eccentricity. The plan dimensions were 50 × 30 m, the dimensions of the center core being 30 × 10 m, and the column spacing (span) being 10 m for all columns. The x-axis was taken to be in the long direction, the y-axis being in the short direction, and the z-axis being in the vertical direction. **Figure 2(a)** and **2(b)** shows the elevation and plan views of the frame model. Steel braces (blue members in **Fig. 2(a)** and **2(b)**) that resist horizontal forces are attached to the center core, the shape of the core causing stiffness differences in the two horizontal directions.

The member material was assumed to be SN490—that is, a steel material used for building structures—with a box-shaped cross-section, the dimensions of which are shown in **Table 1** with reference to [18]. In consideration of the in-plane stiffness of the floor slab, rigid horizontal braces (light blue members in **Fig. 2(b)**) were inserted in the floor structure, the total mass calculated from the dimensions of the members being 2.30×10^7 kg. A fixed load of 4,700 N/m^2—excluding the weight of the member itself—was assumed, considering the weight of the reinforced concrete slab, etc. [19]. The live load for calculating the seismic force of an office building was assumed to be 800 N/m^2, based on Article 85 of the Building Standard Law Enforcement Ordinance. The masses calculated from these loads are distributed to the beams as follows: first, multiplying the 50 × 30 m plan and the number of stories by 50 yields a total of 4.21×10^7 kg. This mass is distributed evenly across the beam at a ratio of 1:5 between the core section (30 × 10 m) and the other sections. Furthermore, assuming a curtain wall [20], 5.60 $\times 10^7$ kg is equally distributed to the beams at the perimeter. Consequently, the total weight of the building model is 1.21×10^8 kg.

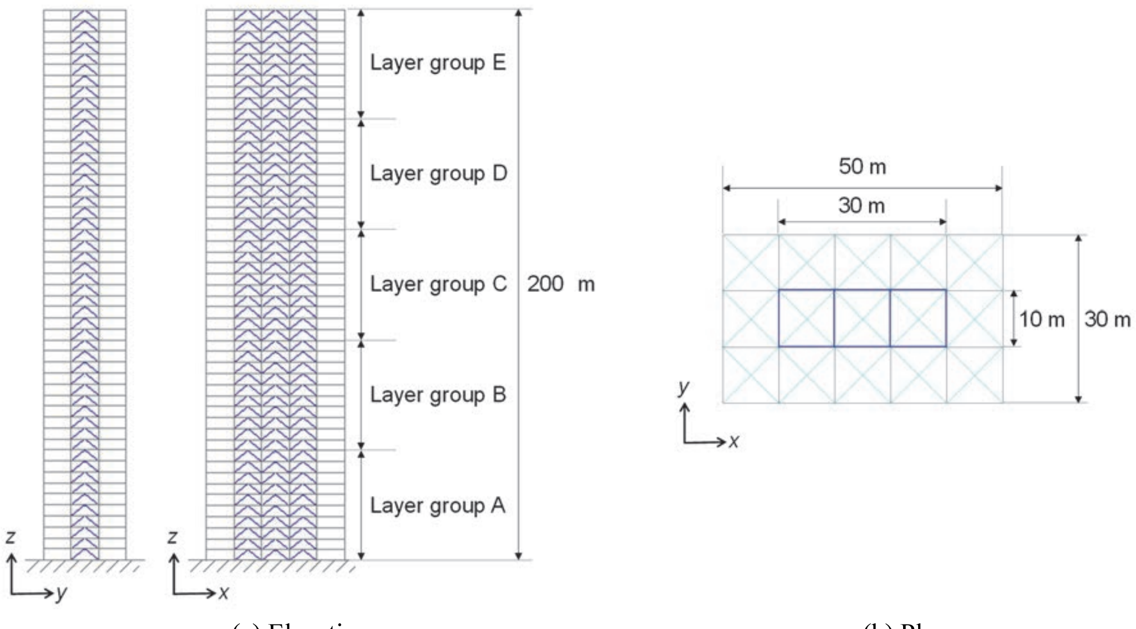

(a) Elevation (b) Plan

Figure 2: The three-dimensional frame model of a high-rise building.

Member		Dimension [mm]
Column	Group A	1000 × 1000 × 50
	Group B	1000 × 1000 × 45
	Group C	1000 × 1000 × 40
	Group D	1000 × 1000 × 36
	Group E	1000 × 1000 × 30
Beam		BH-1000 × 400 × 19 × 40
Brace		500 × 500 × 25

Table 1: The dimensions of members.

2.2 Vibration characteristics of the model

We performed a modal analysis of the frame model described in the previous section. The ANSYS Workbench Mechanical 2021 R2 finite element analysis software was used for the analysis. The columns, beams, and core braces were all modeled using Timoshenko beam elements. The bottom ends of the first-story columns in the frame model were fixed to the ground, the entire frame model then being subjected to gravitational acceleration for analysis.

The vibration characteristics in the translational *x*-, *y*-, and torsional directions (hereafter referred to as the θ-direction) were obtained. **Figure 3** shows the mode shapes in each direction, and **Table 2** summarizes the vibration characteristics—such as the natural frequencies and damping factors. Only the Rayleigh type damping model could be used in the software; the coefficients for the mass matrix (α) and stiffness matrix (β) were set to $\alpha = 1.397 \times 10^{-2}$ s^{-1} and $\beta = 6.328 \times 10^{-3}$ s so that the damping factor for the first modes in the *y*- and θ-directions was 1%. **Table 2** also shows the calculation results for the damping factors of the other modes.

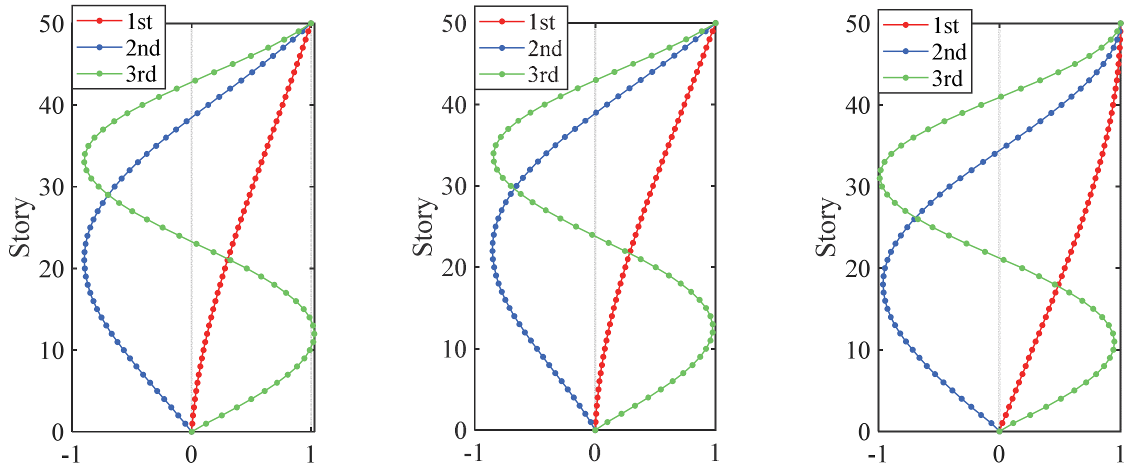

Figure 3: The mode shapes.

Mode	Natural Freq. [Hz]	Natural Circular Freq. [rad/s]	Natural Period [s]	Damping Factor [%]
1st *x*-direction	0.239	1.499	4.193	0.940
2nd *x*-direction	0.907	5.699	1.102	1.926
1st *y*-direction	0.166	1.042	6.031	1.000
2nd *y*-direction	0.741	4.657	1.349	1.623
1st θ-direction	0.337	2.119	2.966	1.000
2nd θ-direction	0.980	6.159	1.020	2.062

Table 2: The vibration characteristics.

In previous studies [9, 17] different Q–Δ resonance conditions have been derived, as shown in **Table 3**. Focusing on the natural frequencies of the translational modes in **Table 2**, the sum of the natural frequencies of the first mode in the x-direction and the second mode in the y-direction is 0.980 Hz. The natural frequency of the second mode in the θ-direction is also 0.980 Hz, which is close to the sum in the translational direction within an error of 0.1%—including those to the fourth decimal place. Consequently, the frame model in this study satisfies the resonance condition of C4, as shown in **Table 3**, and the torsional response can be expected to increase when the first-order mode in the x-direction and the second mode in the y-direction are excited. Based on the measured damping database [16] of the Architectural Institute of Japan, we investigated whether real buildings in Japan satisfied the Q–Δ resonance conditions shown in **Table 3** and found that a particularly large number of buildings satisfied the C4 and C6 resonance conditions. Consequently, the natural frequencies of the frame model used in this study can be considered to be close to the characteristics of real buildings in Japan.

Condition Name	Condition	Condition Name	Condition
C1	$f_{\theta 1} = f_{x1} + f_{y1}$	C9	$f_{\theta 1} = \lvert f_{x1} - f_{y1} \rvert$
C2	$f_{\theta 2} = f_{x1} + f_{y1}$	C10	$f_{\theta 2} = \lvert f_{x1} - f_{y1} \rvert$
C3	$f_{\theta 1} = f_{x1} + f_{y2}$	C11	$f_{\theta 1} = \lvert f_{x1} - f_{y2} \rvert$
C4	$f_{\theta 2} = f_{x1} + f_{y2}$	C12	$f_{\theta 2} = \lvert f_{x1} - f_{y2} \rvert$
C5	$f_{\theta 1} = f_{x2} + f_{y1}$	C13	$f_{\theta 1} = \lvert f_{x2} - f_{y1} \rvert$
C6	$f_{\theta 2} = f_{x2} + f_{y1}$	C14	$f_{\theta 2} = \lvert f_{x2} - f_{y1} \rvert$
C7	$f_{\theta 1} = f_{x2} + f_{y2}$	C15	$f_{\theta 1} = \lvert f_{x2} - f_{y2} \rvert$
C8	$f_{\theta 2} = f_{x2} + f_{y2}$	C16	$f_{\theta 2} = \lvert f_{x2} - f_{y2} \rvert$

Table 3: Q–Δ resonance conditions in terms of natural frequencies [9]; the first subscript of the natural frequency f indicates the direction of vibration, the second subscript indicating the mode order.

3 TIME-HISTORY RESPONSE ANALYSIS OF THE MODEL

A time-history response analysis was performed by inputting seismic motion to a frame model of a high-rise building using the vibration characteristics described above. The members were assumed to be linearly elastic, and geometric nonlinearity was considered to investigate the occurrence of Q–Δ resonance. In the analysis, the bottom ends of the first-story columns were fixed to the ground and the entire frame model was subjected to gravity and ground motion acceleration. The input ground motions included the design waves OS1 and CH1 [21], which were long-period seismic ground motions developed by the Ministry of Land, Infrastructure, Transport and Tourism for structural design purposes, with a time step of 0.02 s. To provide ground motions in two horizontal directions, each design wave was input in a direction 45° from the x-axis direction—that is, waves with an amplitude scaled by cos 45° were input in both the x- and y-axis directions. The acceleration time history of the OS1 and CH1 design waves are shown in **Fig. 4(a)** and **4(b)**, respectively. In the time-history response analysis, time intervals of 50–230 s for OS1 and 70–250 s for CH1 were extracted (each duration: 180 s), as shown in **Fig. 4(a)** and **4(b)**, respectively—denoted by the shaded blue background—and input into the model. The absolute acceleration and displacement response spectra for an input wave with a damping factor of 1%, extracted from the above time interval and scaled by cos 45°, are shown in **Fig. 4(c)** and **4(d)**, respectively. The natural periods of the first and second modes in each direction are also shown in the figures.

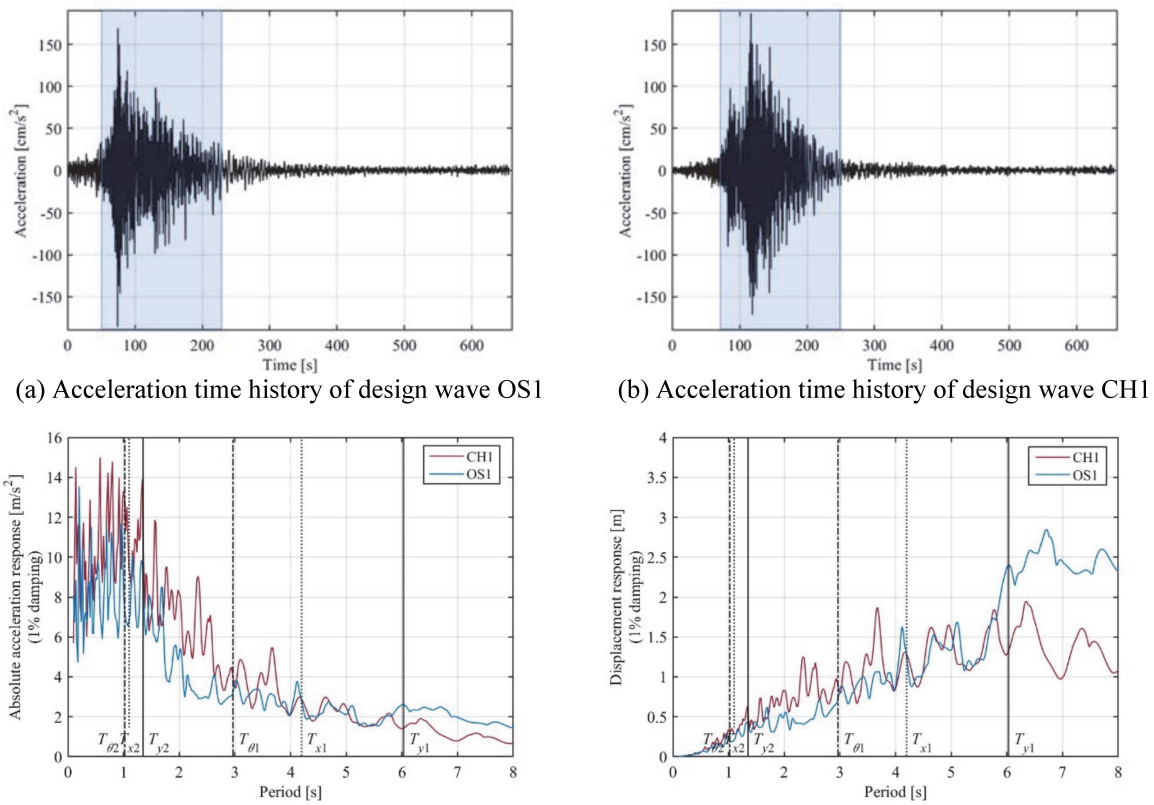

(a) Acceleration time history of design wave OS1 (b) Acceleration time history of design wave CH1

(c) Absolute acceleration response spectra (d) Displacement response spectra

Figure 4: The input ground motions and their response spectra.

Figure 5 shows the displacement and absolute acceleration responses in each direction at the center of the top slab, obtained from the time-history response analysis. In the frame model, the damping factors of the first mode in the *y*- and *θ*-directions are set to 1%. The target building does not have a supplemental structure—such as outriggers—to suppress translational displacement other than the center core. As shown in **Fig. 5(a)** and **5(c)**, the translational displacement at the top slab is particularly large in the *y* (weak axis)-direction.

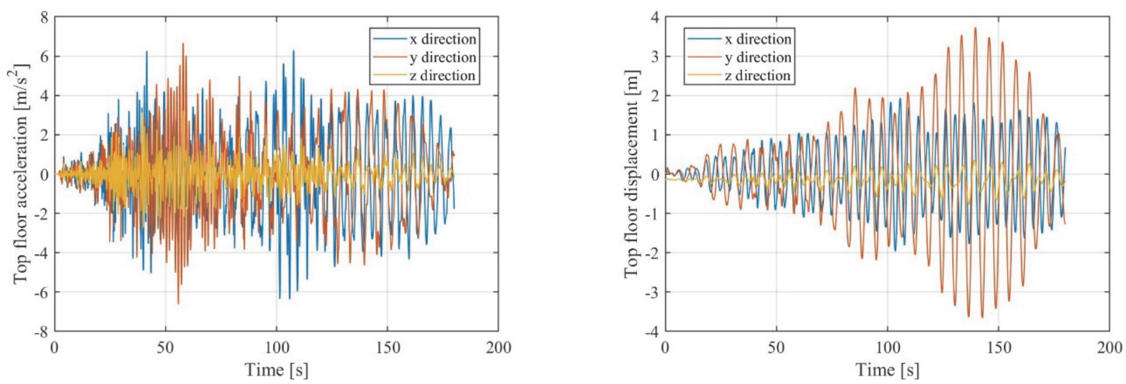

(a) Absolute acceleration response to OS1 (b) Displacement response to OS1

Figure 5: Analytical results of the translational responses.

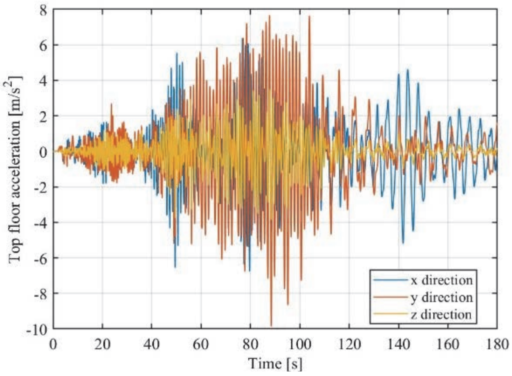

(c) Absolute acceleration response to CH1

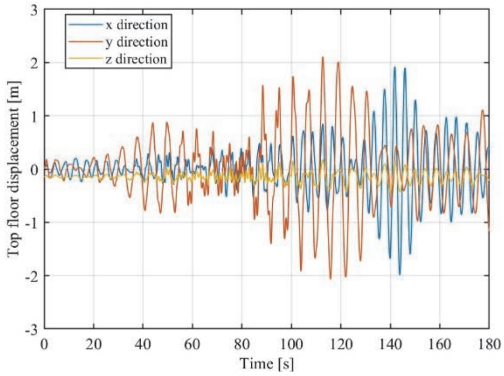

(d) Displacement response to CH1

Figure 5: Analytical results of the translational responses (continued).

The torsional displacement and angular acceleration responses at the center of the top slab can be calculated from the translational responses of the two diagonal upper corner points of the slab. The corner displacements of the top slab can be defined as (x_1, y_1) and (x_2, y_2), as shown in **Fig. 6**. The distance between the center and each corner of the slab are given by $r = (r_x^2 + r_y^2)^{1/2}$, where the x- and y-directional distances r_x = 25 m and r_y = 15 m. The torsional displacement and angular acceleration responses at the center of the slab can then be calculated using the translational acceleration at the corners of the slab as follows:

$$\theta = \frac{1}{2r^2}(-r_y x_1 + r_y x_2 + r_x y_1 - r_x y_2) \tag{1}$$

$$\ddot{\theta} = \frac{1}{2r^2}(-r_y \ddot{x}_1 + r_y \ddot{x}_2 + r_x \ddot{y}_1 - r_x \ddot{y}_2) \tag{2}$$

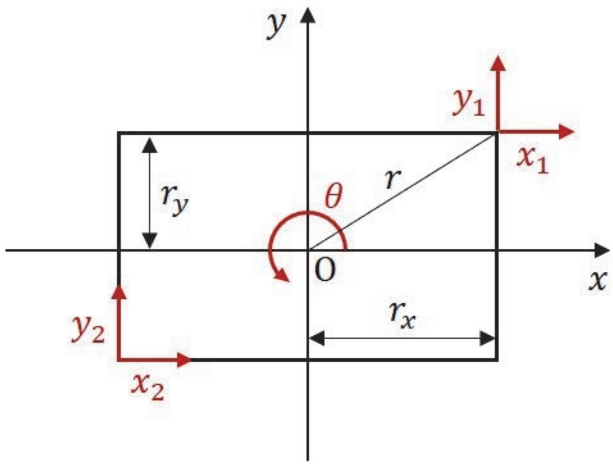

Figure 6: The symbols used in the calculation of torsional responses.

The obtained torsional displacements and angular accelerations at the center of the top slab are shown in **Fig. 7(a)–7(d)**. As is evident from **Fig. 7(a)** and **7(b)**, the analytical result of the OS1 wave yields a maximum torsional angle of 0.04° and a maximum angular acceleration of 5×10^{-3} rad/s^2. Similarly, the analytical result of the CH1 case yields a maximum torsional angle of 0.01° and a maximum angular acceleration of 3×10^{-3} rad/s^2, as shown in **Fig. 7(c)** and **7(d)**.

When the maximum horizontal absolute acceleration response at the corners of the slab (A_{Cmax})—that is, the maximum with respect to both time and the four corners—is larger than that at the center of the slab (A_{Gmax}), the ratio $A_{\mathrm{Cmax}}/A_{\mathrm{Gmax}}$ increases. Consequently, $A_{\mathrm{Cmax}}/A_{\mathrm{Gmax}}$ can be used as an index to measure the torsional response owing to Q–Δ resonance. Calculating the ratio from the results of this study, we obtain 1.014 and 1.005 for the OS1 and CH1 cases, respectively. These results indicate that the horizontal absolute acceleration at the corner of the top layer increases by a maximum of 1.4% and 0.5%, respectively.

As shown in **Table 1**, this analytical model assumes square cross-section columns in accordance with ordinary buildings. However, even when square cross-section columns with no stiffness difference in the two translational directions are used, a stiffness difference in the two horizontal directions due to the shape of the center core can cause torsional response owing to Q–Δ resonance.

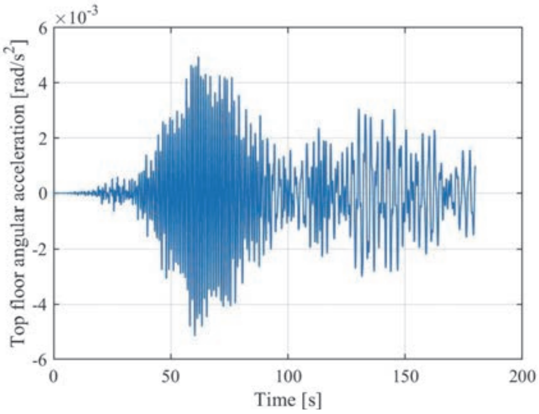

(a) Angular acceleration response to OS1

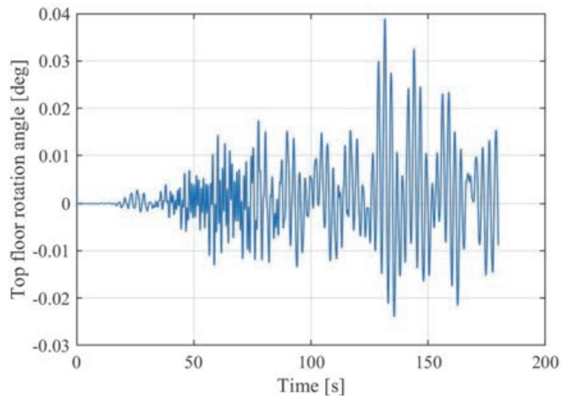

(b) Torsional displacement response to OS1

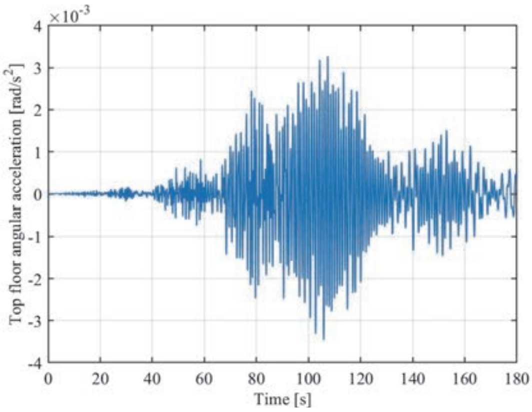

(c) Angular acceleration response to CH1

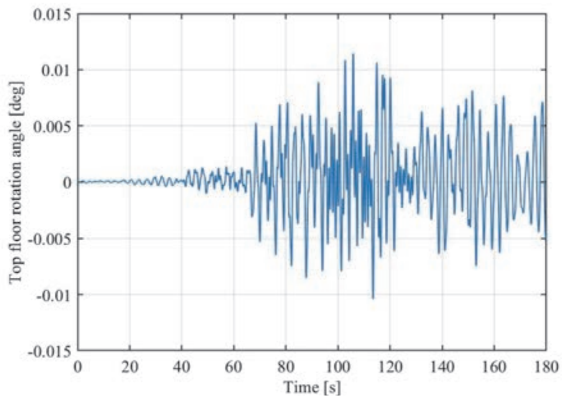

(d) Torsional displacements response to CH1

Figure 7: Analytical results of the torsional responses.

4 CONCLUSIONS

A three-dimensional frame model of a center-core high-rise building satisfying the Q–Δ resonance condition in the second torsional mode was developed, and a time-history response analysis was conducted considering geometric nonlinearities. The analytical results using long-period design waves OS1 and CH1 as input ground motions showed a stimulus of the torsional response and increase in horizontal absolute acceleration at the corners of the slab, confirming that the torsional response emerged owing to the Q–Δ resonance in a building with a biaxially symmetrical plan.

In this study, Rayleigh damping was used in the analytical model, which was characterized by a larger damping factor for higher-order modes; 1.62% for the second y-direction mode and 2.06% for the second torsional mode, as shown in **Table 2**. However, actual high-rise buildings also have damping factors of approximately 1% in higher-order modes. Additionally, the material properties were assumed to be linear elastic, and the increase in damping due to yielding was not considered.

Consequently, we should set up an appropriate damping model and consider material nonlinearities for more accurate predictions of the response of high-rise buildings. Furthermore, we could accurately verify the risk of earthquake damage due to Q–Δ resonance in real buildings by conducting analyses using models that satisfy other resonance conditions, as shown in **Table 3**, than the C4 condition assumed in this study. Future work should include derivation of a theory considering the interaction of the P–Δ and Q–Δ effects and accurate verification of the risk of seismic damage due to Q–Δ resonance in real buildings.

ACKNOWLEDGMENT

This research was financially supported by SECOM Science and Technology Foundation and JSPS Grant-in-Aid for Scientific Research (B) No. 20H02301.

REFERENCES

[1] S.A. Anagnostopoulos, M.T. Kyrkos, K.G. Stathopoulos, Earthquake induced torsion in buildings: Critical review and state of the art. *Earthquakes and Structures*, **8**, 305–377, 2015.

[2] A.M. Chandler, G.L. Hutchinson, Torsional coupling effects in the earthquake response of asymmetric buildings. *Engineering Structures*, **8**, 222–236, 1986.

[3] R.K. Goel, Seismic behaviour of asymmetric buildings with supplemental damping. *Earthquake Engineering and Structural Dynamics*, **29**, 461–480, 2000.

[4] G.K. Georgoussis, An alternative approach for assessing eccentricities in asymmetric multi-story buildings: 1. Elastic systems. *The Structural Design of Tall and Special Buildings*, **18**, 181–202, 2009.

[5] M. Kohiyama, H. Yokoyama, Torsional response induced by lateral displacement and inertial force. *Frontiers in Built Environment*, **4**, Article 38, 2018.

[6] H. Yokoyama, F. Mizutori, M. Kohiyama, "Q–Δ resonance," resonance phenomenon of torsional response induced by inertial force perpendicular to horizontal displacement. *Proceedings of the 66th Structural Engineering Colloquium of Architectural Institute of Japan Kinki Branch*, 2019. (in Japanese)

[7] R. Anamizu, F. Mizutori, M. Kohiyama, Validation experiment of Q–Δ resonance in the second torsional mode reproduction analysis using finite element model. *Proceedings of the Annual Meeting of Japan Association for Earthquake Engineering*, Paper ID: A-2-1, 2020. (in Japanese)

[8] R. Anamizu, F. Mizutori, M. Kohiyama, Fundamental study on Q–Δ resonance considering second mode in a non-eccentric structure. *Summaries of Technical Papers of Annual Meeting Architectural Institute of Japan*, **Structure II**, 463–464, 2020. (in Japanese)

[9] R. Anamizu, M. Kohiyama, Fundamental study of Q–Δ resonance considering higher-order modes by shaking table experiments and finite element analysis. *Journal of Structural Engineering*, Architectural Institute of Japan, **68B**, 386–396, 2022. (in Japanese)

[10] M. Kohiyama, H. Yokoyama, S. Maki, Torsional response of a bisymmetric structure induced by bending-torsion interaction in vertical members. *Japan Architectural Review*, **5**, 3–19, 2022.

[11] S. Maki, M. Kohiyama, Torsional behavior of a non-eccentric structure considering the effect of shear deformations in vertical members. *Japan Architectural Review*, **5**, 404–431, 2022.

[12] F. Mizutori, H. Yokoyama, M. Kohiyama, Experiment on torsional response of symmetric structure induced by Q–Δ resonance. *Proceedings of the 17th World Conference on Earthquake Engineering*, Sendai, Japan, Paper ID: 2c-0204, 2020.

[13] F. Mizutori and M. Kohiyama, Experiment of torsional response induced by the Q–Delta resonance. *The Structural Design of Tall and Special Buildings*, **30**, e1829, 2021.

[14] F. Mizutori, Study on Q–Δ resonance of super high-rise building using shaking table test and finite element analysis. *Master Thesis of School of Science for Open and Environmental Systems, Graduate School of Science and Technology, Keio University*, 2021. (in Japanese)

[15] T. Watanabe, M. Nagano, K. Kato, Influence of accretionary wedge along the Nankai Trough and earthquake locations on long-period ground motions in Tokyo. *Journal of Structural and Construction Engineering*, **79**, 701–710, 2014.

[16] Architectural Institute of Japan, *Database of Actual Vibration Measurements of Various Buildings and Structures (December 2020)*, http://news-sv.aij.or.jp/kouzou/s7/d1, accessed on March 5, 2022. (in Japanese, title translated by the authors)

[17] R. Anamizu, Study on simplified model of high-rise building for evaluating Q–Δ resonance using shaking table test and finite element analysis. *Master Thesis of School of Science for Open and Environmental Systems, Graduate School of Science and Technology, Keio University*, 2022. (in Japanese)

[18] Nippon Steel Corporation, *Dimensions and properties of Hyper Beam®, Handbook of Nippon Steel Construction Materials*, April 2019 Edition, https://www.nipponsteel.com/product/construction/handbook/pdf/3-20.pdf, accessed on March 5, 2022. (in Japanese)

[19] JFE Steel Corporation, Chapter 2: Load and stress combinations, *Steel Structure Design Handbook*, 2-1–2-21, https://www.jfe-steel.co.jp/products/building/assets/pdf/binran/binran_all.pdf, accessed on March 5, 2022. (in Japanese, title translated by the authors)

[20] K. Kabayama, K. Kusunoki, Chapter 1: General matters, *Hitori-de Manaberu RC-zou Kenchikubutsu-no Kouzou Keisan Enshucho* (Exercise book for structural calculation of RC buildings that you can learn by yourself), The Building Center of Japan, p. 22, https://www.bcj.or.jp/publication/html/bcj_upload/product_file/101_04_RCWEB2.pdf, accessed on March 5, 2022. (in Japanese, title translated by the authors)

[21] Building Research Institute, Special webpage for the release of technical information and data related to measures against long-period ground motion, https://www.kenken.go.jp/japanese/contents/topics/lpe/index.html, accessed on March 5, 2022. (in Japanese)